ADVANCED SURFACE MICROMACHINING PROCESS – A FIRST STEP TOWARDS 3D MEMS

Johannes Classen[1], Jochen Reinmuth[1], Arnd Kälberer[1], Andreas Scheurle[1], Sebastian Günther[1], Stefan Kiesel[1], Bernt Schellin[1], Jörg Bräuer[1], and Laura Eicher[2]
[1]Robert Bosch GmbH, Automotive Electronics, Reutlingen, GERMANY
[2]Bosch Sensortec GmbH, Reutlingen, GERMANY

ABSTRACT

An advanced micromachining process has been developed to further push the performance limits of mass-produced inertial MEMS. The main achievement of the new platform technology is the usage of two independent silicon layers instead of one to form, e.g., masses, springs, and free-standing electrodes. This dual layer process option opens the path towards new 3D-like sensor topologies with improved performance and smaller form-factors. The first accelerometer generations using this technology are being manufactured for automotive and CE applications. One of the key features of these new devices is their unparalleled offset stability which they maintain even in stress-affected mold packages.

INTRODUCTION

Surface micromachining is a well-established method for the mass-production of MEMS inertial devices [1, 2, 3]. Alternatively, wafer bonded device layers [4, 5] or SOI based technologies are used for mass-production of silicon based inertial sensors. The approaches of all major industrial players of recent years have in common that the inertial sensors are manufactured using a single thick micromechanical silicon layer (typically 10 – 30 µm) for the movable structures. Additional silicon or metal layers are being used only for wiring and fixed electrodes to sense out of plane movements. A first approach to free-standing multi-layer structures has been demonstrated by Freescale where fully suspended vias between a thick functional and a thin wiring layer were realized [6]. However, even in this approach the movable structure was built only from the thick layer.

Significant progress has been made with respect to process optimization, manufacturing tolerances, design improvements, and packaging technologies to bring down cost and form factor of the sensors and to push at the same time their performance and quality levels [7, 8, 9]. Nevertheless, due to the design constraints of the single layer processes and with new demanding requirements for automotive and CE applications on the horizon, the standard MEMS technologies are approaching their limits. In this paper we present an advanced dual layer MEMS process which enables more sophisticated sensor designs and allows to reach very ambitious performance targets.

ADVANCED SURFACE MICRO-MACHINING PROCESS

The standard Bosch MEMS surface micromachining process used for mass-production of billions of capacitive inertial sensors served as a basis for the new technology development. The standard process essentially consists of a thin buried poly-silicon layer for wiring and out of plane capacitive detection and a thick poly-silicon layer for the actual micromechanical structure (masses, springs, etc.). The two silicon layers are separated by a sacrificial oxide layer, which is partially removed by HF vapor phase etching to realize fully released MEMS structures.

In the new process an additional micromechanical silicon layer of intermediate thickness and an additional sacrificial oxide layer were integrated in the process flow. The additional micromechanical layer is arranged between the wiring layer and the thick silicon layer. The three poly-silicon layers will be denoted as P1 (wiring), P2 (additional layer), and P3 (thick top layer). Because only P2 and P3 will be used for free-standing MEMS structures, we will refer to the new process as "dual layer MEMS process".

One of the major obstacles in multi-layer processes is the avoidance of topography in lower layers for the subsequent process steps of the upper layers. The problem is particularly serious when the layers are fairly thick, i.e., in the range of several micrometers. While in the CMOS world the topography issue is solved by successive CMP steps we have chosen a different approach using a two-stage structuring of the P2 layer [10]. This provides much more freedom of design and better scalability with respect to layer thickness.

The process flow of the new dual layer process is schematically shown in Fig. 1. It starts with forming an oxide layer O1 on the wafer substrate, deposition and structuring of the P1 wiring layer and of a sacrificial oxide layer O2. Afterwards the P2 layer is deposited. With the first mask for P2 only narrow DRIE trenches are defined, as shown in Fig 1a). Afterwards an oxide layer O3a is deposited, which covers the sidewalls of the trenches and seals the trenches at the top side almost without topography. The oxide layer is structured with a fine grid only and serves as the second mask for P2. An isotropic SF6 etch is done and stops at the oxide-covered P2 sidewalls (Fig. 1b). By this procedure large sacrificial areas of P2 can be removed although the oxide mask has only tiny openings. Next, an oxide layer O3b is added which fills the small holes of the O3a layer almost without topography, i.e., leaves a basically flat area for the subsequent P3 deposition even in areas where P2 was widely carved out. Before P3 deposition, contact holes in O3a, O3b are formed for mechanical and electrical contact between P2 and P3. The rest of the process sequence basically corresponds to the standard Bosch surface micromachining process, namely deposition (Fig. 1c) and DRIE of P3 and release of the MEMS structures by a timed vapor phase HF etch (Fig. 1d). The P2 layer can be etched independently of or together with the thick P3 layer, i.e., the etch mask of the P3 layer is the third option to structure the P2 layer.

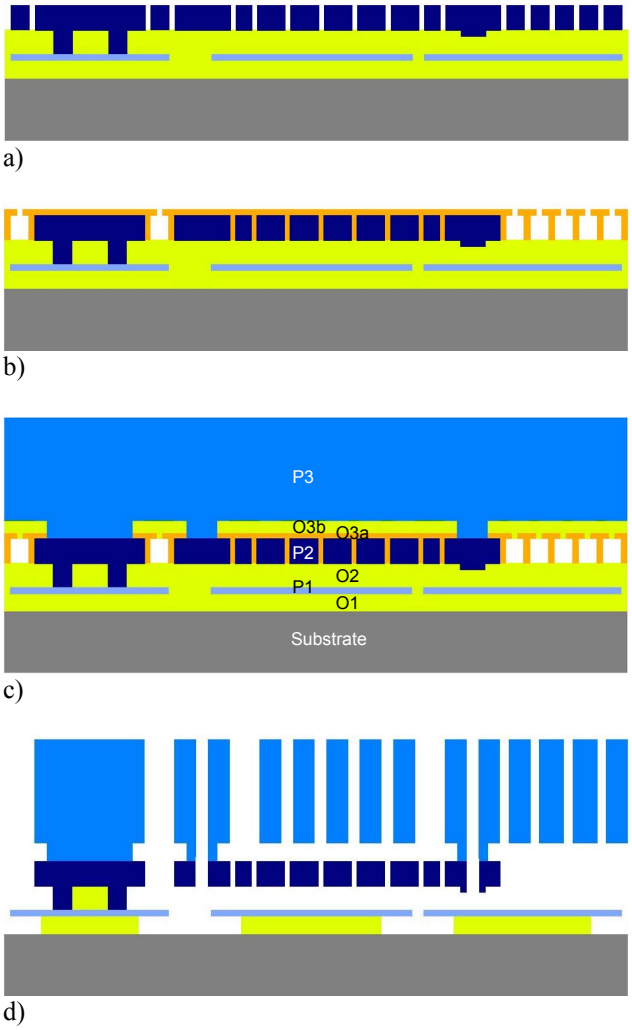

Figure 1: Sketch of the process flow of the dual layer MEMS process. Image c) contains the labeling of the layer stack.

DESIGN TOPOLOGIES

The process sequence of the dual layer MEMS process provides enormous flexibility in MEMS design and enables new sensor topologies, especially free-standing 3D-like structures for masses and electrodes which are very well decoupled from mechanical stress occurring in the package and hence in the MEMS substrate.

Figure 2 depicts a bird's view sketch of a torsional rocker-type z-accelerometer which can be designed in the dual layer MEMS process [11]. The movable structure is formed from the P2 and partially from the P3 layer. Moreover, the sensor has a double differential electrode arrangement, i.e., not only C1 and C2 electrodes for differential signal readout, but both bottom and top C1 (green) and C2 (red) electrodes. Top electrodes built from the P3 layer are anchored very closely to the fixation of the movable mass and hence are only weakly affected by substrate bending. In addition, due to the double differential electrode configuration, the bottom electrodes can be made smaller and put closer to the central anchoring of the movable structure without sacrificing overall sensitivity of the device. As a result of the electrode arrangement, the whole structure is very compact and widely insensitive to packaging stress and thus provides superior offset stability.

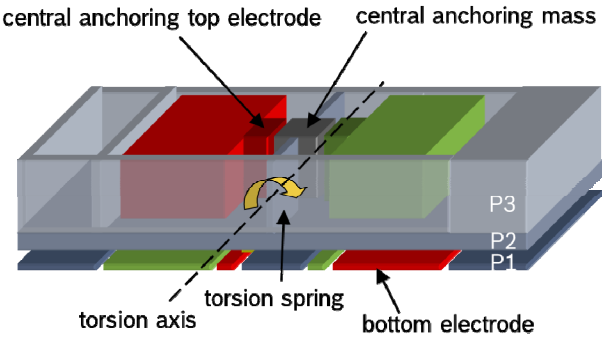

Figure 2: Sketch of the new design topology of the z-accelerometer

Moreover, the sensor has an open tub-like structure on the very left of the movable structure which provides a highly symmetric interface (with respect to the torsional axis) between the P1 wiring layer and the bottom P2 surface of the movable structure. As a consequence, parasitic effects from the bottom surface, e.g., due to electrostatic forces from trapped surface charges on the P1 layer, balance out very well. This improves the offset stability of the device even further. At the same time, the mechanical sensitivity due to the difference of the moments of inertia on both sides of the torsional spring is almost entirely maintained, because on the left side the P3 layer is widely removed. This combination of high electrical symmetry but high mechanical asymmetry requires 3D-like process options and cannot be achieved by standard single layer MEMS processes. Figure 3 is a SEM picture of a processed sample.

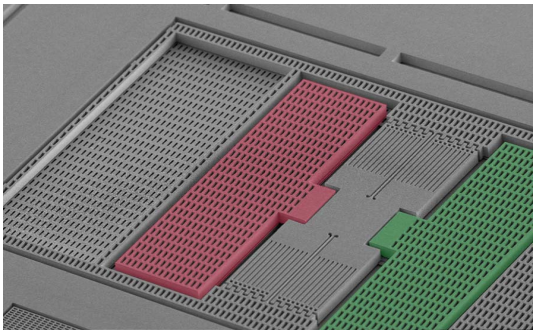

Figure 3: SEM picture of a z-accelerometer with the new design topology. Fixed top electrodes have been colorized for clarity. On the left side of the movable structure the tub-like structure built from P2 and P3 can be seen.

The dual layer MEMS process can also be used to achieve major improvements for x-/y-accelerometers [12]. Figure 4 shows a colorized SEM picture of a x-accelerometer. Only the P3 layer is well visible here. The movable structure is colored blue, and fixed C1, C2 electrodes are colored green and red, respectively. Grey areas mark the fixation and the mechanical over-travel stops (small areas at bottom and top) of the movable

structure. All mechanical anchorings to the substrate (except for the over-travel stops) are located in the center region marked by the orange-dotted rectangle covering less than 10% of the total area of the sensor. The rest of the structure is fully released and is therefore very well decoupled from substrate deformation due to package stress.

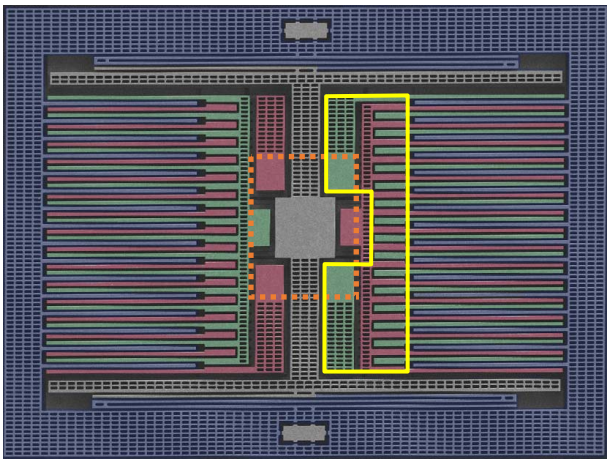

Figure 4: Colorized SEM picture of a x-accelerometer. The central anchoring region of mass and electrodes is marked with orange dots, and the outline of one of the underetched P2 plates used for fixation of the P3 electrodes is shown as yellow line.

Central fixation of movable structures and fixed electrodes is well-known for many years as a good recipe against package stress [13, 14]. It has been widely used in several mass-produced accelerometer generations of, e.g., STMicroelectronics and Bosch, to improve the offset performance of the sensors. However, in contrast to the sensors above, the design presented here combines central anchoring of mass and electrodes with differential electrode cells. From the basic idea this is similar to the Freescale approach mentioned in the introduction [6] but the technical realization is very different.

As can be easily seen by the color coding of Fig. 4, for every movable (blue) electrode there is an opposing green C1 and red C2 electrode. This is possible because, e.g., on the right hand side of Fig. 4 the green C1 electrodes realized in P3 are fixed on a P2 plate which is fully underetched (except for the two central anchorings in the orange-dotted area) and underbridges the red C2 electrodes which are realized only in P3. For clarity, the outline of the right P2 plate is marked as yellow line.

The combination of central fixation and differential electrode cells is again enabled by the new dual layer MEMS process because the sensor topology of Fig. 4 is based on the capability of realizing free-standing crossings and via connections of two MEMS layers. The design topology not only optimizes the offset stability but also increases the sensitivity of the device (or allows to shrink the device and preserve the sensitivity). Moreover, the damping is increased which is usually very desirable for accelerometers to improve their vibration immunity.

Figure 5 shows a more detailed SEM picture of part the central fixation area of a different x-accelerometer sample. Clearly visible here is the complex arrangement of the three poly-silicon layers P1, P2, and P3.

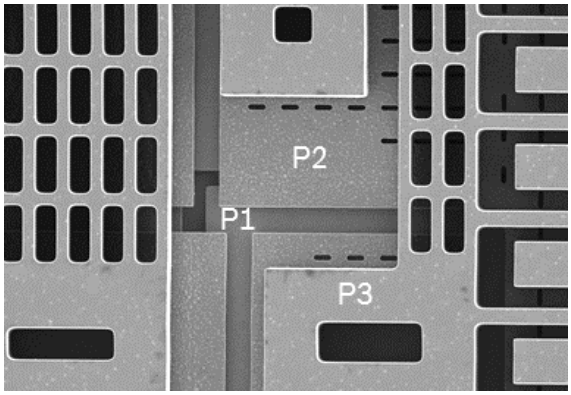

Figure 5: SEM picture of part of the central anchoring region of a x-accelerometer fabricated in the dual layer MEMS process.

EXPERIMENTAL RESULTS

One of the main targets of the new technology and design concepts was the improvement of the offset stability of both x-/y- and z-accelerometers. Mechanical stress is known to be one of the dominant contributions to offset errors in present mass-produced accelerometers. It is particularly critical in cost-efficient mold packages widely used for automotive and CE applications, e.g., due to mismatch of the thermal expansion coefficients of the different materials, plastic deformation of the mold compound due to ageing, and hygro-swelling upon exposure to humid environments [15].

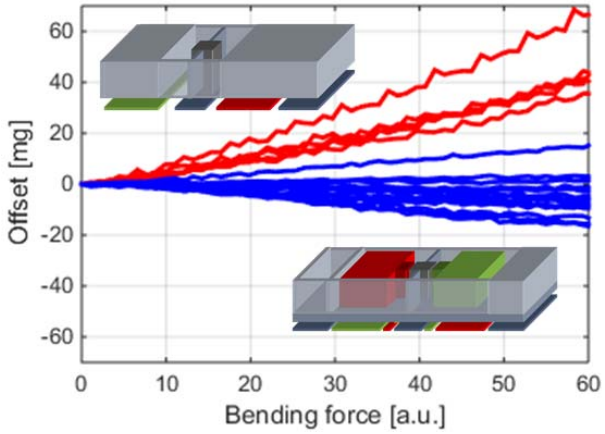

Figure 6: Offset shift as a function of bending force for five samples with standard rocker design (red lines, upper sketch) and eleven samples with the new z-accelerometer design (blue lines, lower sketch)

Figure 6 shows the result of a bending experiment where sensors soldered to a PCB were subjected to well-defined mechanical deformation. The red lines refer to five samples of a standard rocker design (i.e., using only one thick micromechanical layer and fixed bottom electrodes in the wiring layer) while the blue lines refer to eleven samples of the new design topology according to Fig. 2. For all sensors there is an almost linear correlation

between bending force and offset error but for the new design the errors are reduced roughly by a factor of 4. This experiment directly demonstrates the strongly enhanced immunity against mechanical stress of the new designs.

In Fig. 7 a comparison is made between the offset stability over temperature (incl. drift effects from soldering to a PCB) of standard x- and z-accelerometers (19 parts) and samples manufactured using the advanced dual layer MEMS technology (40 parts). All sensors were packaged in the same LGA housing and used the same ASIC. Moreover, chip size and thickness were identical. Despite the significantly larger number of parts, the distribution of offset errors is much narrower for the new designs. Here the improvement both for solder drift (i.e. in Fig. 7, offset values at room temperature) and TCO is approximately a factor of 3 compared to the standard designs. It is remarkable how large the improvement even for the x-accelerometer is because the reference design used here had already a central anchoring of the seismic mass and of the fixed electrodes but was missing the differential electrode cells. Standard x-accelerometers with differential electrode cells but without central anchoring would typically have an even inferior performance as compared to the reference design of Fig. 7.

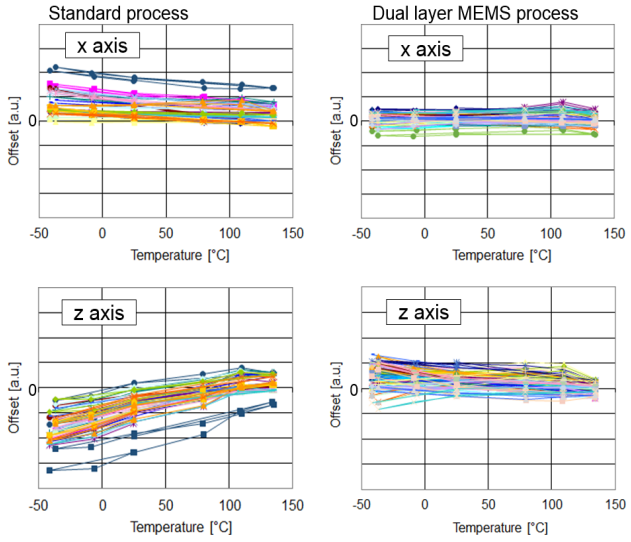

Figure 7: Offset vs. temperature for accelerometers manufactured in the standard Bosch surface micromachining process (left column, 19 parts) and sensors with the new design topologies produced in the dual layer MEMS process (right column, 40 parts). Upper row for x-axis, lower row for z-axis.

The mass-production of inertial sensors with the advanced dual layer MEMS process was started in 2015 for automotive applications (vehicle dynamics control, hill-hold control) for the accelerometers of the inertial sensors SMI700 and SMI710 [16]. Figure 8 shows an image of the BGA64 (7x7 mm²) package of the device. Despite the stress-affected mold package the accelerometers exhibit excellent offset stability.

Figure 8: BGA64 package of the most recent family of Bosch inertial sensors for vehicle dynamics control.

For CE applications the first sensor using the dual layer MEMS process is the three-axis accelerometer BMA455 from Bosch Sensortec [17]. It is in final development phase, mass-production will start soon. Figure 9 shows an image of the LGA package of the device with dimensions 2x2x0.65 mm³. The low thickness of the package requires significant thinning of the MEMS sensors and would usually make it more susceptible to mechanical stress and hence cause inferior offset performance. However, due to the dual layer MEMS process the BMA455 has a benchmark offset stability reaching maximum TCO values for all three axes of 0.5 mg/K. Also, drift effects from soldering to PCB are reduced to a minimum.

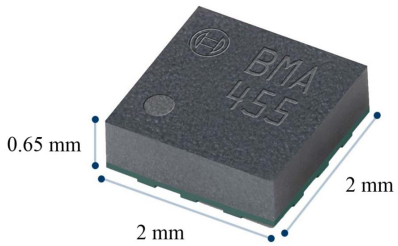

Figure 9: LGA package of the first CE accelerometer using the advanced dual layer MEMS process.

OUTLOOK

The dual layer MEMS process is an enabler for a large variety of new design elements for future MEMS products. It can be used, e.g., for complex wiring as well as for new spring, mass, and membrane designs. It is also possible to stack several independent devices on a single chip [18]. Applications are by no means restricted to accelerometers but may also be extended to gyroscopes and, with some additional process steps, to capacitive pressure sensors [19].

One of the major advantages of the process is its scalability with respect to two aspects. Firstly, the thickness of the P2 layer can be chosen in a wide range of values. For the first product generations a small thickness of only a few micrometer was used. However, it is in principle possible to extend the layer thickness to significantly larger values of, e.g., 10 – 20 µm without major changes in the generic process flow. As an example, Figure 10 shows a SEM image of a demonstrator device with P2 thickness of 10 µm. Part of the MEMS structure was pulled out to make the thick P2 layer visible.

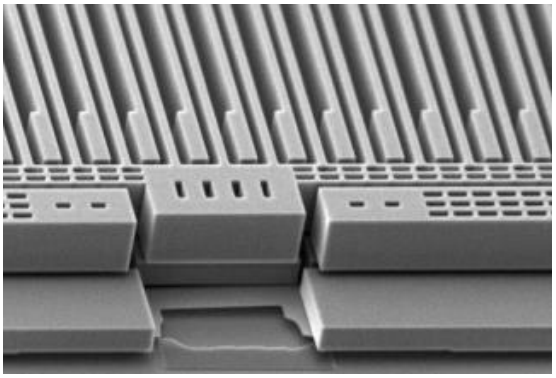

Figure 10: SEM picture of a sample with 10 µm thick P2 layer visible after removal of part of the structure.

Secondly, due to the avoidance of topography, multi-layer stacks of polysilicon can be in principle piled up and may thus enable the path to even more complex 3D MEMS structures. It is conceivable that such process options may be used to further push performance limits of inertial sensors. It is obvious, though, that additional layers will add wafer cost and yield penalties. Therefore, although fascinating by itself from an academic point of view, the path to more complex 3D silicon structures will only be paved once new demanding requirements for existing high-volume applications come up or compelling ideas for new applications and products emerge.

REFERENCES

[1] STMicroelectronics, http://www.st.com/content/en/about/innovation---technology/mems.html

[2] A. M. Reze, J. Hammond, in "Advanced Microsystems for Automotive Applications 2005", Springer, Berlin, 2005, pp 459-471.

[3] F. Lärmer, A. Schilp, K. Funk, M. Offenberg, in Proc. IEEE MEMS 1999, Orlando, USA, pp. 211-216.

[4] S. Nasiri, Whitepaper, "A critical review of MEMS gyroscopes technology and commercialization status" Invensense, 2012.

[5] mCube Whitepaper, 2014, www.mcubemems.com/wp-content/uploads/2014/06/mCube-Advantages-of-Integrated-MEMS-Final-0614.pdf.

[6] A. Geisberger *et al.*, in Proc. TRANSDUCERS 2013, Barcelona, Spain, pp. 18-21.

[7] U.-M. Gomez *et al.*, in Proc. TRANSDUCERS 2005, Seoul, South Korea, vol. 1, pp. 184-187.

[8] STMicroelectronics, Technical article TA0343, http://www.st.com/resource/en/technical_article/dm00034730.pdf.

[9] C. D. Ezekwe, W. Geiger, T. Ohms, in Proc. IEEE ISSCC 2015, San Francisco, USA, Session 27.3., pp. 1-3.

[10] J. Reinmuth, H. Weber, Patent US 8,659,099 B2.

[11] J. Classen, Patent Application US 2010/0175473 A1.

[12] J. Classen, C. Bierhoff, Patent US 8,443,671 B2.

[13] S. J. Dixon-Warren, MEMS Journal, Dec. 23, 2010, http://www.memsjournal.com/2010/12/motion-sensing-in-the-iphone-4-mems-accelerometer.html

[14] P. Sulzberger, M. Offenberg, Patent US 5,983,721 A.

[15] J. B. Kwak, S. Park, Microelectronics International, (2015) Vol. 32 Issue 1, pp. 8-17.

[16] Robert Bosch GmbH, Automotive Electronics, http://www.bosch-semiconductors.de/en/automotive_electronics/mems/vehicledynamicssystems/vehicle_dynamics_systems.html

[17] Bosch Sensortec GmbH, https://www.bosch-sensortec.com/bst/products/motion/accelerometers/overview_accelerometers

[18] J. Classen, Patent Application US 2011/0056295 A1.

[19] A. Kälberer, J. Reinmuth, J. Classen, Patent Application US 2015/0008542 A1.

CONTACT

*J. Classen, tel: +49-7121-354929;
johannes.classen@de.bosch.com